J Seismol (2018) 22:1595–1612
https://doi.org/10.1007/s10950-018-9788-z

ORIGINAL ARTICLE

Interdependent quality control of collocated seismometer and accelerometer

Izidor Tasič

Received: 12 May 2017 / Accepted: 20 August 2018 / Published online: 4 September 2018

Abstract A new method for the interdependent quality control (IQC) of a collocated seismometer and accelerometer is presented. It is useful for seismic stations, where broadband seismometer and strong-motion accelerometer are installed side by side. The number of this type of seismic stations is growing and so is the number of activities associated with the quality control. With the IQC, the collocated seismometer and accelerometer are controlled with the single procedure. It is based on the calculation of transformation matrix which numerically transforms the detection of a seismic signal of accelerometer to the space of detection of seismometer. This matrix contains a lot of information; among them were also the "orientation misalignment," "sensitivity corrections," and two indicators, from which the quality of data and the error of systems can be identified. The procedure uses seismic signals, detected by both systems. The self-noise of commercial accelerometers is usually higher than the average seismic noise; therefore, a moderate shaking of the ground is needed. This type of shaking can come from stronger regional earthquakes. In this article, a mathematical description of the procedure is introduced first; then, a few examples with real data are presented. A critical error was discovered with the help of this algorithm. It cannot be identified by testing signals, injected from an acquisition unit into the STS-2 seismometer. There is also an example of serious orientation misalignment between a seismometer and an accelerometer.

I. Tasič (✉)
Slovenian Environment Agency, Vojkova 1b, 1000 Ljubljana, Slovenia
e-mail: izidor.tasic@gov.si

Keywords Seismometer · Accelerometer · Side-by-side installation · Quality control · Error identification · Orientation misalignment · Sensitivity · Gain constant

Abbreviations

PSD	Power spectral density
CPSD	Cross-power spectral density
3D	Three dimensional
IQC	Interdependent Quality Control
NLNM	New Low Noise Model (Peterson 1993)

1 Introduction

The number of seismic stations, where a broadband seismometer and a strong-motion instrument known as accelerometer are installed side by side, is rising. The main reason for placing these instruments together is to increase the dynamic range of observation as the strong ground motion could clip the record of a seismometer. Modern broadband seismometers are very sensitive to weak seismic signals and are capable to detect small local events or weak signals from distant earthquakes. As for strong-motion signals, they are too sensitive and can be clipped. On the other hand, the accelerometers are insensitive to weak seismic signals but are not clipped in case of strong movements of the Earth.

In the case of moderate shaking of the ground, the seismometer signals are not clipped and the accelerometer is also capable to properly detect this movement. When the source of shaking is distant enough, both

systems should detect equal movement of the ground. After the processing of the recorded digital signals on computers, the outputs from the both systems should give the same information (e.g., estimated ground motion).

Due to various reasons, the output can differ. The following three main causes of unequal detection are the differences related to the accuracy of calibration data, the errors resulting from misalignment of two collocated systems, and the errors resulting from the defects of a particular system.

The error mentioned first originates from differences in data calibration files of various manufacturers. The physical outputs of measuring units are voltages. Seismometer outputs are proportional to the velocity of ground movement and accelerometer outputs are proportional to its acceleration. Proportional coefficients, usually known as "gain constants" of seismometers and "sensitivity" of accelerometers, are given in instrumental calibration sheets. The steps for obtaining and verifying these values are not standardized among the producers of seismic equipment. There are also differences in the calibration data files. Some manufacturers provide generic values. As example of this is "STS-2 certificate of calibration," where the generator constants for X, Y, and Z components are written as "1500 ± 15 [V/(m/s)] each." Some manufactures give absolute values for each component. For example, in the calibration sheet of CMG-5TC accelerometer, responses are written to three decimal places for each component. The design of calibration sheets is not standardized; therefore, small variations in the evaluated amplitudes of the same ground movement between two different systems can exist. Variations can be larger, if calibration data are incorrectly entered into the parameter file of software in the data processing center.

The second source of error is due to the different orientation of these two systems. Some small misalignment errors in the size of a tenth of degree can always be expected. The error in the parallel orientation may become larger, when both systems are not installed at the same time, or the defects of a particular system may cause temporary reinstallation, where careless handling can cause unidentified movements of instrument. This is quite possible, when some works are performed in a narrow deep vertical shaft in the presence of external negative distractions such as rain showers.

The third source of error is the defects of a particular system. This is always critical, if the defects are not identified during the routine analysis of waveforms, the daily controls, and inspections. The errors are not easily recognizable when they cause only small deviations from the expected waveforms. An example of this is the electro corrosion between the pins of the connector, which can cause a change in conductivity. It may occur because of a long-lasting use in a humid environment at the military type of connectors, due to small irregularities of the contacts. Unidentified errors can cause an incorrect interpretation of the results.

With the interdependent quality control (IQC) of collocated seismometer and accelerometer, all three types of errors can be identified and also minimized. Some examples are presented in the Sections 3 and 4.

Side-by-side installation of two or more seismometers has been studied by many researchers (e.g., Pavlis and Vernon 1994; Holcomb 1989, 1990, 2002; Wielandt 2002; Sleeman et al. 2006; Ringler and Hutt 2010; Sleeman and Melichar 2012; Tasič and Runovc 2012, 2013, 2014; …). The input signal for these studies is ambient seismic vibration, which can be detected everywhere on a free surface anytime. This type of a signal is not appropriate for accelerometers as their self-noise is usually above the New Low Noise Model (NLNM; Peterson 1993) at almost over the whole frequency range (Ringler et al. 2015). For this reason, a moderate shaking of the ground is needed for the study of both collocated instruments, where a seismometer signal is not clipped yet, whereas the accelerometer is capable to detect it. The ground shaking must be the same for both systems (Tasič and Runovc 2012), and it is usually a result of stronger regional or moderate local earthquakes. The advantage of regional earthquakes is in longer duration of shaking. Seismic signals from these sources usually exist in the frequency range between 0.2 and 0.5 Hz, where transfer functions of broadband seismometers and of force balanced accelerometers are flat (Collette et al. 2011).

Mathematical description of the procedure will be presented in Section 2. It will be seen that with the process of IQC, the inputs are the data that do not need to be converted to different physical units. In Sections 3 and 4, some examples will be presented, including the example of different errors being identified. In Sections 5 and 6, discussion and conclusion are presented.

2 Collocated seismometer-accelerometer

The IQC of collocated seismometer-accelerometer is based on the relation of detected seismic signals from both systems. The following mathematical description of the

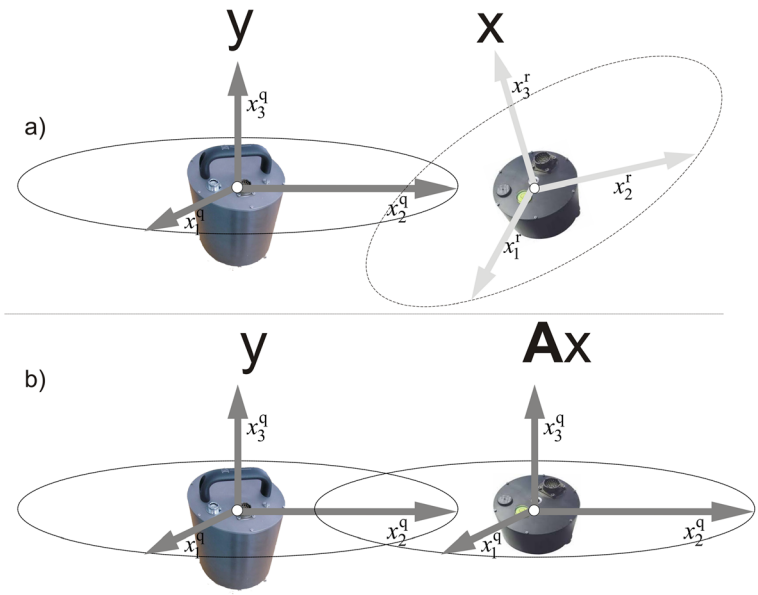

Fig. 1 Three-component broadband seismometers "q" and three-component accelerometer "r" are placed side by side, but they are not having equal orientation, their gains are not the same, etc. **a** Both systems detect ground motion in their own coordinate systems, system "r" and system "q." **b** The transformation matrix **A** maps the detection of accelerometer into the space of seismometer detection; after the transformation, both systems detect ground motion in coordinate system "q"

model is presented first as a one-dimensional approach where two linear systems, representing seismometer and accelerometer, are both fed by a common input signal. The output y_q of the seismometer "q" is the convolution of the input signal x with the instrumental transfer-function h_q adding the internal noise n_q (Tasič and Runovc 2012):

$$y_q^{(\text{velocity})} = h_q \otimes x + n_q. \tag{1}$$

The output y_r of the accelerometer "r" is the convolution of the input signal x with the accelerometer transfer-function h_r and the instrumental internal noise n_r:

$$y_r^{(\text{acceleration})} = h_r \otimes x + n_r. \tag{2}$$

The output power spectral density (PSD) for the seismometer "q," on the assumption that the system is linear and the noise is completely uncorrelated, can be expressed by the following:

$$\mathrm{P}_{qq} = H_q H_q^* \mathrm{P}_{xx} + \mathrm{N}_{qq}, \tag{3}$$

where * denotes the complex conjugation and $\mathrm{P}_{xx} = XX^*$ is the autopower spectrum of the common input signal (Sleeman et al. 2006). Replacing the index "q" with "r" yields the PSD expression for the accelerometer. As P_{qq} represents the velocity power spectral density value, one can calculate the respective values of the acceleration power spectral density (Borman 2002) as

$$\mathrm{P}_{qq}^{(\text{acceleration})} = \omega^2 \mathrm{P}_{qq}, \tag{4}$$

By using this relation, the "acceleration" cross-power spectra P_{qr} between the seismometer "q" and the accelerometer "r" can be written as follows:

$$\mathrm{P}_{rq}^{(\text{acceleration})} = \omega \mathrm{P}_{rq} = \omega H_r H_q^* \mathrm{P}_{xx}, \tag{5}$$

As the seismometer and the accelerometer measure the spatial movement of the ground, the three-dimensional (3D) approach will be used (Tasič and Runovc 2012) to identify errors. Assuming that both units provide three signal outputs, they represent mutual orthogonal motions and are marked with indexes 1, 2, and 3. So, if misalignment exists between both measuring systems, such misalignment errors prevent the seismic signal from both systems to be purely coherent (Holcomb 1990). Assuming that the signal x is detected at the seismometer axis "1" only, this is not the case for the accelerometer. Because of misalignment, the output $y_{r_{q1}}$, which represents accelerometer output in the direction x, is a linear combination of accelerometer's partial outputs y_{r1}, y_{r2}, and y_{r3}

$$\begin{aligned} y_{r_{q1}} &= b_{11} y_{r1} + b_{12} y_{r2} + b_{13} y_{r3} \\ &= \sum_{j=1}^{3} b_{1j} \left(h_{jr} \otimes x + n_{rj} \right). \end{aligned} \tag{6}$$

The PSD of $y_{r_{q1}}$ can be written, with the Eqs. (2) and (6), as

$$\mathrm{P}_{\mathrm{r_{q1}r_{q1}}}^{(\mathrm{acceleration})} = \mathrm{P}_{\mathrm{r_{q1}r_{q1}}}(y_{\mathrm{r1}}, y_{\mathrm{r2}}, y_{\mathrm{r3}}, b_{11}, b_{12}, b_{13}), \quad (7)$$

The parameters b_{11}, b_{12}, and b_{13} are unknown and can be estimated by minimizing the "average" of uncorrelated PSD. This procedure is explained in more detail for two collocated seismometers in the Appendix of the article of Tasič and Runovc (2012), and it has been proved in Tasič and Runovc (2014) to be the best for estimating parameters b_{11}, b_{12}, and b_{13}. Therefore, similar modified approach will also be used in the case of collocated seismometer and accelerometer. The goal is to find the transformation matrix that maps the detection of accelerometer into the space of seismometer detection (Fig. 1).

The "average acceleration noise PSD" $\overline{\mathrm{N}}_{ii}$ in the seismometer direction i ($i = 1, 2, 3$), as a function of the frequency ν and parameters $\overrightarrow{b}_{\mathrm{i}} = (b_{\mathrm{i1}}, b_{\mathrm{i2}}, b_{\mathrm{i3}})$, where the seismometer "q" and the accelerometer "r" are installed side by side, by using Eqs. (3), (7), and (5), is governed by the equation

$$\overline{\mathrm{N}}_{ii}\left(\overrightarrow{b}_{\mathrm{i}}, \nu\right) = 0.5\left(4\pi^2\nu^2\mathrm{P}_{\mathrm{q}_i\mathrm{q}_i}(\nu) + \mathrm{P}_{\mathrm{r}_{qi}\mathrm{r}_{qi}}\left(\overrightarrow{b}_{\mathrm{i}}, \nu\right)\right) - \sqrt{4\pi^2\nu^2\mathrm{P}_{\mathrm{q}_i\mathrm{r}_{qi}}\left(\overrightarrow{b}_{\mathrm{i}}, \nu\right)\mathrm{P}_{\mathrm{q}_i\mathrm{r}_{qi}}\left(\overrightarrow{b}_{\mathrm{i}}, \nu\right)}^{*}. \quad (8)$$

The residual vector R for the direction i, at the frequency interval $[\nu_{-n}, \nu_n]$, is as follows:

$$R_i\left(\overrightarrow{b}_{\mathrm{i}}\right) = \left[\overline{\mathrm{N}}_{ii}\left(\overrightarrow{b}_{\mathrm{i}}, \nu_{-n}\right), \ldots, \overline{\mathrm{N}}_{ii}\left(\overrightarrow{b}_{\mathrm{i}}, \nu_n\right)\right]. \quad (9)$$

The values b_{i1},b_{i1}, and b_{i3} can be estimated by minimizing the residue using non-linear least squares methods, where the best fit minimizes the "average acceleration noise PSD". In other words, when $\overline{\mathrm{N}}_{ii}$ consists only of self-noises of both instruments, $\overline{\mathrm{N}}_{ii}$ cannot be lower as it does not contain seismic data and for this reason, estimated values b_{i1}, b_{i1}, and b_{i3} represent the best fit.

When these parameters are determined in all three directions, the 3×3 transformation matrix $\mathbf{B}$ (Tasič and Runovc 2012), which maps the detection of accelerometer into the space of seismometer detection, can be designed

$$\tilde{\mathbf{y}}_{\mathrm{r}} = \mathbf{B}\mathbf{y}_{\mathrm{r}} \rightarrow \begin{bmatrix} \tilde{y}_{1\mathrm{r}} \\ \tilde{y}_{2\mathrm{r}} \\ \tilde{y}_{3\mathrm{r}} \end{bmatrix} = \begin{bmatrix} b_{11} & b_{12} & b_{13} \\ b_{21} & b_{22} & b_{23} \\ b_{31} & b_{32} & b_{33} \end{bmatrix} \begin{bmatrix} y_{1\mathrm{r}} \\ y_{2\mathrm{r}} \\ y_{3\mathrm{r}} \end{bmatrix}. \quad (10)$$

After this transformation, $\tilde{\mathbf{y}}_{\mathrm{r}}$ presents the acceleration data in a new coordinate system, which is aligned with the coordinate system of seismometer. The matrix $\mathbf{B}$ contains information about "sensitivity corrections," about the orientation of the accelerometer regarding the seismometer (misalignment error) and many other data (Tasič and Runovc 2013). It should be noted that matrix $\mathbf{B}$ is very useful in the quality control of seismic instruments. It, directly or indirectly, contains information about the functional failure of systems (Section 4).

The quality of estimated parameters from the matrix $\mathbf{B}$ can be checked by two different indicators. The first indicator is based on a simple trick. If the transformation matrix $\mathbf{B}$, which maps the detection of accelerometer into the space of the detection of seismometer, exists, then also exists the transformation matrix $\mathbf{B_2}$, which maps the detection of seismometer into the space of detection of accelerometer. To calculate the transformation matrix $\mathbf{B_2}$, Eq. (8) is rewritten in the following manner:

$$\overline{\mathrm{N}}_{ii}\left(\overrightarrow{b}_{2\mathrm{i}}, \nu\right) = 0.5\left(4\pi^2\nu^2\mathrm{P}_{\mathrm{q}_{ri}\mathrm{q}_{ri}}\left(\overrightarrow{b}_{2\mathrm{i}}, \nu\right) + \mathrm{P}_{\mathrm{rr}}(\nu)\right) - \sqrt{4\pi^2\nu^2\mathrm{P}_{\mathrm{q}_{ri}\mathrm{r}_i}\left(\overrightarrow{b}_{2\mathrm{i}}, \nu\right)\mathrm{P}_{\mathrm{q}_{ri}\mathrm{r}_i}\left(\overrightarrow{b}_{2\mathrm{i}}, \nu\right)}^{*}. \quad (11)$$

In the absence of any noise, the inv ($\mathbf{B_2}$) should be equal to $\mathbf{B}$. Usually it is not, as the data are not noise-free, and it is also due to the numerical procedure. The elements of matrices $\mathbf{B}$ and $\mathbf{B_2}$ are calculated by using the least squares method on the assumption that the "noise" follows Gaussian distribution and exists only in the response data and not in the target data. But self-noise is frequency dependent (Rodgers 1992) and exists

in both systems. Seismometers and accelerometers are also not ideally linear systems. At larger amplitudes of ground movements, measurements can also be influenced by rotational phenomena, which different sensors record differently (Graizer 2009). The greater is the influence of non-linear phenomena, the more the matrices inv ($\mathbf{B_2}$) and $\mathbf{B}$ differ one from another. The maximal difference between elements of matrices, $\Delta b_{\max} = \max\{|\mathbf{B} - \mathrm{inv}(\mathbf{B_2})|\}$, can be an indicator about the quality of data. Transformation matrices inv ($\mathbf{B_2}$) and $\mathbf{B}$ are similar, if the value $\Delta b_{\max}$ is not "too high." Some examples are shown in Tables 1 and 2.

When this parameter deviates significantly from the expected value, we must pay attention to seismic systems. The example is in Table 3.

The second indicator is a determinant of 3 × 3 transformation matrix $\mathbf{B}_g$. Let $\mathbf{g} = [g_1, g_2, g_3]$, which represents sensitivity corrections for all three components of an accelerometer. The matrix $\mathbf{B}_g$ is obtained by removing the sensitivity corrections from the matrix $\mathbf{B}$:

$$\mathbf{B} = \mathbf{B}_g \cdot \mathbf{g} \rightarrow \begin{bmatrix} b_{11} & b_{12} & b_{13} \\ b_{21} & b_{22} & b_{23} \\ b_{31} & b_{32} & b_{33} \end{bmatrix} = \begin{bmatrix} b_{g11} & b_{g12} & b_{g13} \\ b_{g21} & b_{g22} & b_{g23} \\ b_{g31} & b_{g32} & b_{g33} \end{bmatrix} \begin{bmatrix} g_1 \\ g_2 \\ g_3 \end{bmatrix}. \quad (12)$$

On the assumption that sensitivity corrections are correctly calculated and all axes of sensors are orthogonal, the matrix $\mathbf{B}_g$ should represent pure rotation and $|\det(\mathbf{B}_g)|$ should be 1. Because of the numerical background of the procedure and the non-orthogonality of components, the actual value of $|\det(\mathbf{B}_g)|$ is practically never 1. However, small deviations are not critical, as will be presented in Section 3. An example of the critical value of determinant is presented in Table 3; its explanation is in Section 4 and indicates irregularities in data. Matrix $\mathbf{B}_g$ also contains data about relative non-orthogonality of accelerometer sensors (Tasič and Runovc 2013), but that is beyond the scope of this paper. It is only important to know that small deviations, few tenths of a degree, do not affect the results.

In the following, we will assume that the self-noise of the acquisition unit is always well below of the self-noise of the accelerometer. To evaluate the self-noise of accelerometer in the presence of moderate seismic signal, as the self-noise of accelerometer is relatively high in comparison with the self-noise of broadband seismometer (Ringler et al. 2015), the following approximation can be used:

$$\mathrm{N}_{\mathrm{r}_i\mathrm{r}_i} = \mathrm{P}_{\mathrm{r}_{qi}\mathrm{r}_{qi}} - \frac{\mathrm{P}_{\mathrm{r}_{qi}\mathrm{q}_i}\mathrm{P}_{\mathrm{r}_{qi}\mathrm{q}_i}^{*}}{\mathrm{P}_{\mathrm{q}_i\mathrm{q}_i}} \text{ if } \mathrm{P}_{\mathrm{q}_j\mathrm{q}_j}, \mathrm{P}_{\mathrm{r}_i\mathrm{r}_i} > \mathrm{N}_{\mathrm{q}_i\mathrm{q}_i} \quad (13)$$

The constant $4\pi^2\nu^2$ from Eqs. (4) and (5) is equal in the numerator and the denominator and is canceled out. The same expression is valid also in cases with two collocated seismometers, where the self-noise PSD of the tested seismometer is higher than that of reference seismometer (Tasič and Runovc 2012). Thus, the obtained self-noise PSD of accelerometer must be equivalent to the self-noise PSD, which is obtained from the acceleration data in the time period of a lower seismic activity.

3 Examples

Examples from three seismic stations with station codes SKDS, GROS, and BOJS will be presented. The seismic station GORS is 85 km north from SKDS, and the seismic station BOJS is located 90 km south from SKDS. At all locations,

Table 1 At the seismic station SKDS, STS-2 seismometer and EpiSensor are installed side by side and both connected to the Q330HRS acquisition unit. The IQC of collocated seismometer and accelerometer was performed on four records of regional earthquakes. The following parameters are presented: "sensitivity corrections" ($\mathbf{g} = [g_{EW}\ g_{NS}\ g_Z]^T$), misalignment error ($\alpha^{(\circ)}$), the difference in (vertical) leveling ($|\theta|^{(\circ)}$), indicator $|\det(\mathbf{Bg})|$, and indicator $\Delta b_{\max}$

Date of the earthquake	Mw	g_{EW}	g_{NS}	g_Z	α	$\lvert\theta\rvert$	$\lvert\det(\mathbf{B}_g)\rvert$	$\Delta b_{\max}$
2016 August 24	6.2	0.986	0.986	0.988	−0.33°	0.50°	1 + 4e−6	8e−05
2016 October 26	6.1	0.987	0.986	0.988	−0.33°	0.51°	1 + 5e−6	7e−05
2016 October 30	6.5	0.987	0.985	0.987	−0.39°	0.52°	1 + 2e−6	4e−05
2017 January 18	5.7;5.6	0.987	0.986	0.986	−0.34°	0.57°	1 + 7e−6	2e−04

Table 2 The seismic station GORS is equipped is with the CMG-3T seismometer, EpiSensor, and Q330HRS acquisition unit. The same parameters as in the Table 1 are presented

Date of the earthquake	Mw	g_{EW}	g_{NS}	g_Z	α	$\lvert\theta\rvert$	$\lvert\det(\mathbf{B}_g)\rvert$	Δb_{max}
2016 August 24	6.2	0.991	0.983	0.994	1.32°	0.39°	1 + 9e−6	1e−04
2016 October 26	6.1	0.991	0.984	0.995	1.28°	0.44°	1 + 13e−6	7e−05
2016 October 30	6.5	0.991	0.984	0.995	1.30°	0.40°	1 + 10e−6	1e−04
2017 January 18	5.7; 5.6	0.989	0.982	0.993	1.30°	0.41°	1 + 9e−6	1e−04

seismometers and accelerometers were installed side by side and connected to a six-channel Q330HRS acquisition units.

Between August 2016 and January 2017, a few regional earthquakes with epicenters in central Italy caused moderate shaking at the location of these seismic stations. From these events, four records were suitable for the IQC (Fig. 2). The three waveform records comprised the data of three earthquakes with a magnitude over 6 (Mw). The fourth waveform data includes two earthquakes with the magnitudes 5.7 and 5.6. Both events occurred consecutively on January 2017 (Fig. 2).

Figures 3 and 4 present 15 min period of all four records from both systems (seismometer and accelerometer) at the station SKDS. The records of the particular event (e.g., "October 26, 2016") have the same length and the start time (Fig. 5 and 6), regardless of the seismic station. The lengths of records for different events are not the same. The shortest is 19 min and 30 s (record "January 18, 2017"), the longest is 60 min (record "October 30, 2016"), the record "August 24, 2016" is 20 min long, and the record "October 26, 2016" is 40 min long. The record length for each event was chosen more or less randomly. As we will show later, the choice of the length of the record is not so critical in the process of calculating the parameters. It is important to state that in the frequency interval where the calculations are performed, the PSD of recorded seismic signal is at least 20 dB above the instrumental noise of a noisier instrument. Therefore, the length of the record can be determined by algorithms based on the signal-to-noise ratio. Unless otherwise stated, all seismic data, used in calculation, were sampled at 200 samples per second. Matlab© built-in functions were used in all calculations (www.mathworks.com). For PSD estimation, the "cpsd" function (using the Welch's (1967) averaged, modified periodogram method) is used with a Hanning window of length to obtain eight equal sections of input data with 50% overlapping time-series segments. All transformation matrices were calculated in the frequency range between 0.2 and 0.5 Hz (Tasič and Runovc 2012). For better presentation, all PSD plots are smoothed. PSD plot of accelerometer, unless otherwise stated, will always represent data, which are transformed into the space of seismometer. The instrument response corrections were not used in any calculations or in PSD graphs.

At the seismic station SKDS, the seismometer STS-2 and the accelerometer EpiSensor (the last one manufactured in the year 2000) are installed side by side in a 4-m deep shaft. Figure 7 presents a record of an earthquake that originated in central

Table 3 The seismic station BOJS: the seismometer STS-2 and the EpiSensor are installed side by side; both are connected to the Q330HRS acquisition unit. The "IQC" identified the defect at the system (line 2, italics). The source of the error was seismometer cable. During the replacement process, the seismometer was shifted slightly (line 3, italics) and soon after it was reoriented

Date of the earthquake	Mw	g_{EW}	g_{NS}	g_Z	α	$\lvert\theta\rvert$	$\lvert\det(\mathbf{B}_g)\rvert$	Δb_{max}
2016 August 24	6.2	0.984	0.985	0.986	3.00°	0.47°	1 + 14e−6	1e−4
2016 October 26	6.1	*0.573*	0.984	0.986	*5.14°*	0.65°	*1 + 1278e−6*	*1e−3*
2016 October 30	6.5	0.983	0.986	0.986	*11.35°*	0.56°	1 + 9e−6	1e−4
2017 January 18	5.7;5.6	0.984	0.985	0.986	− 1.64°	0.55°	1 + 24e−6	2e−04

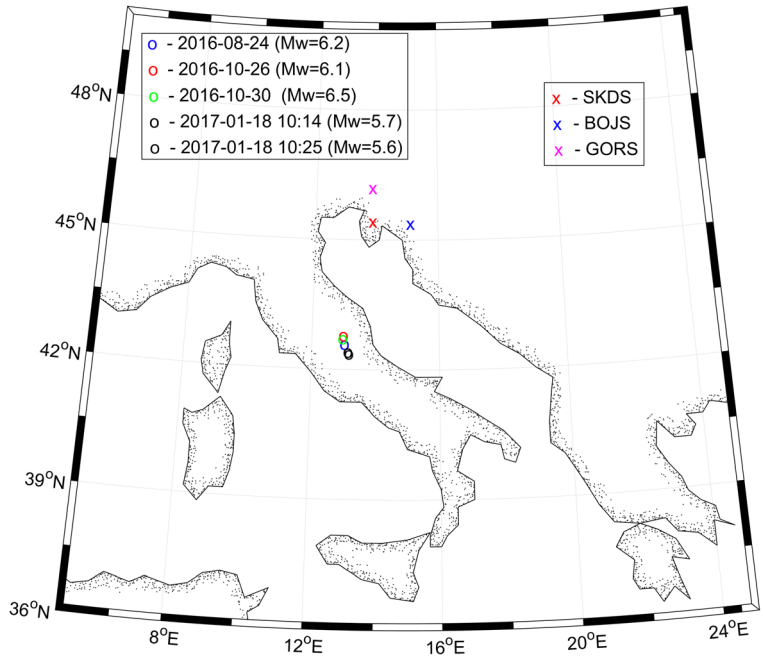

Fig. 2 The efficiency of the "interdependent quality control" (IQC) of collocated seismometer and accelerometer was demonstrated at three seismic stations (labels "x"). For each seismic station, four IQC were performed with different earthquake records (labels "o"). The fourth record contains two earthquakes which occurred on a same day (January 18, 2017), in a short time sequence

Italy (October 30, 2016, Mw = 6.5). The distance of the seismic station from the earthquake epicenter is 308 km. The following IQC was based on this data. The 3×3 transformation matrix **B** that maps the

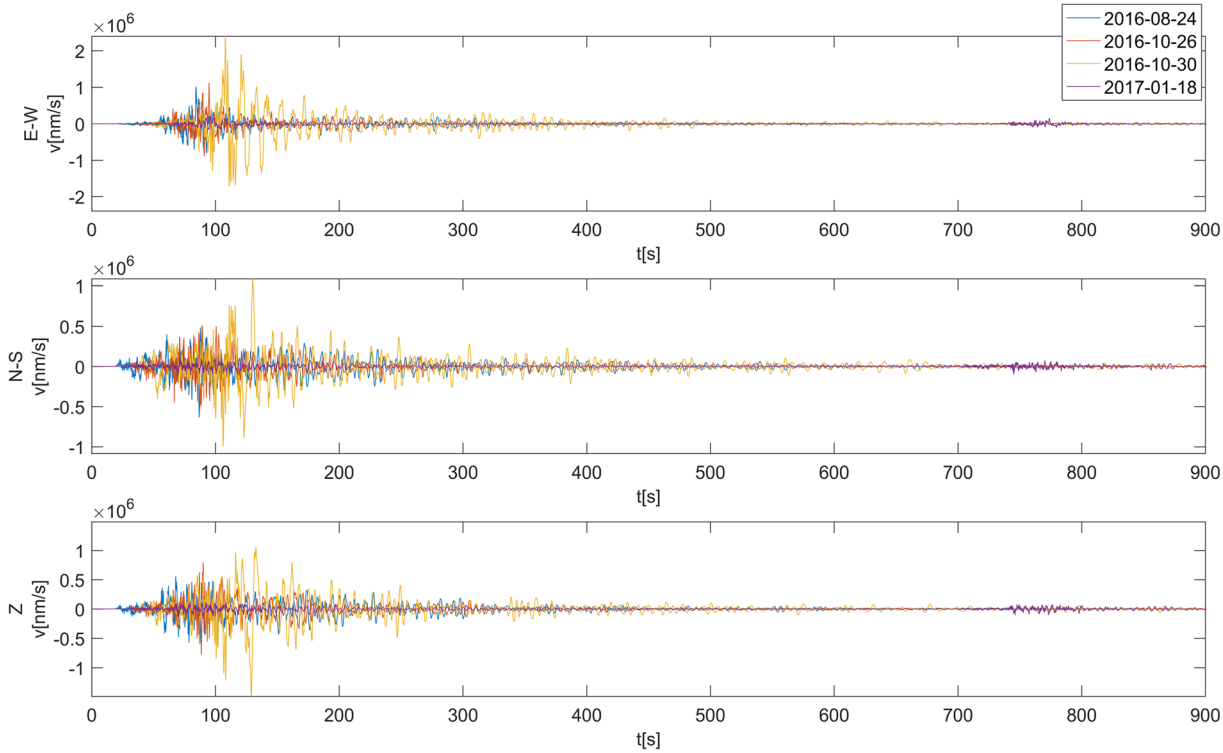

Fig. 3 This figure compares four different records from the station SKDS recorded by seismometer STS-2, which were used for the IQC of collocated seismometer and seismometer. First 15 min of waveforms is presented only

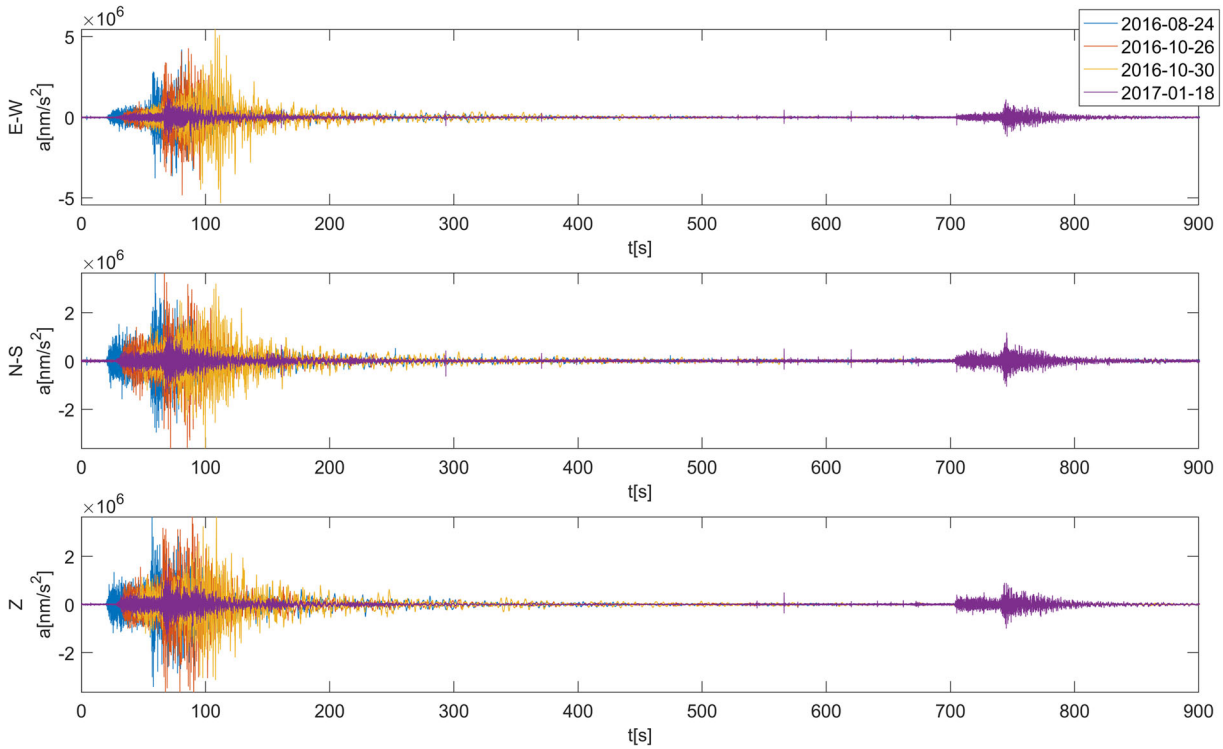

Fig. 4 As in Fig. 3, only the data are recorded with the accelerometer EpiSensor

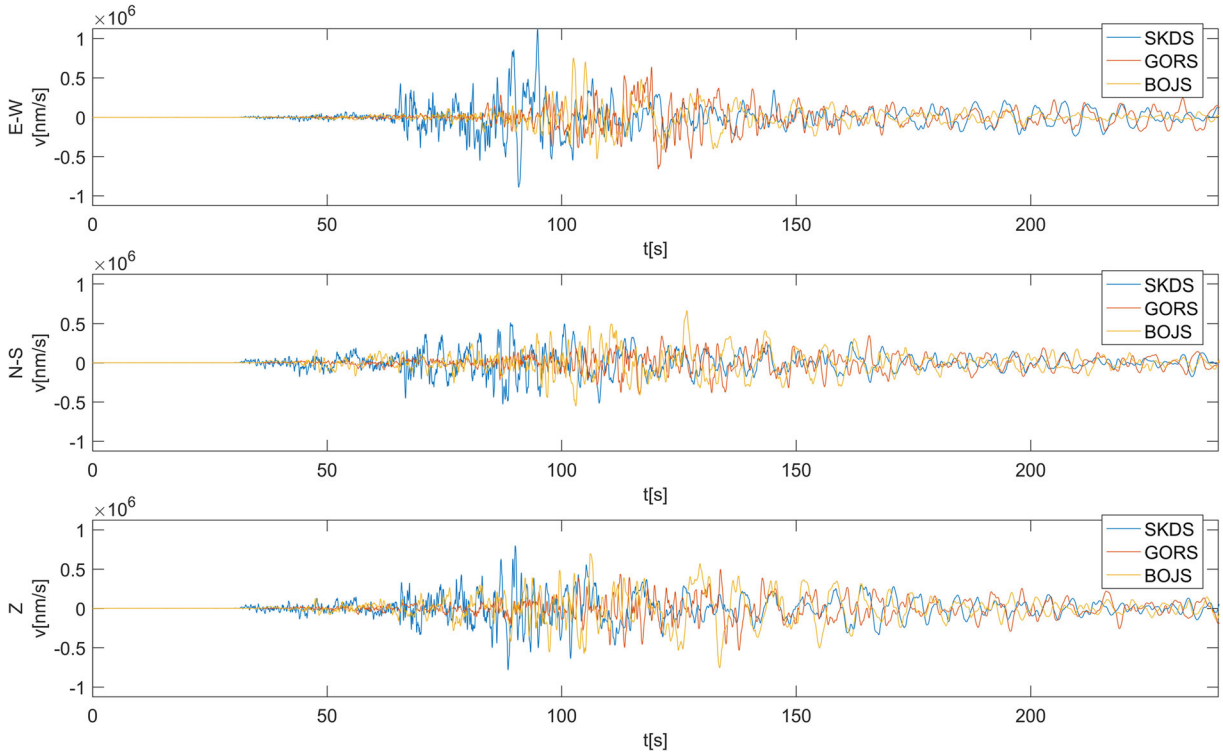

Fig. 5 This figure compares seismometer records (first 4 min) for the event "October 30, 2016" from three different sites (SKDS, GORS, BOJS)

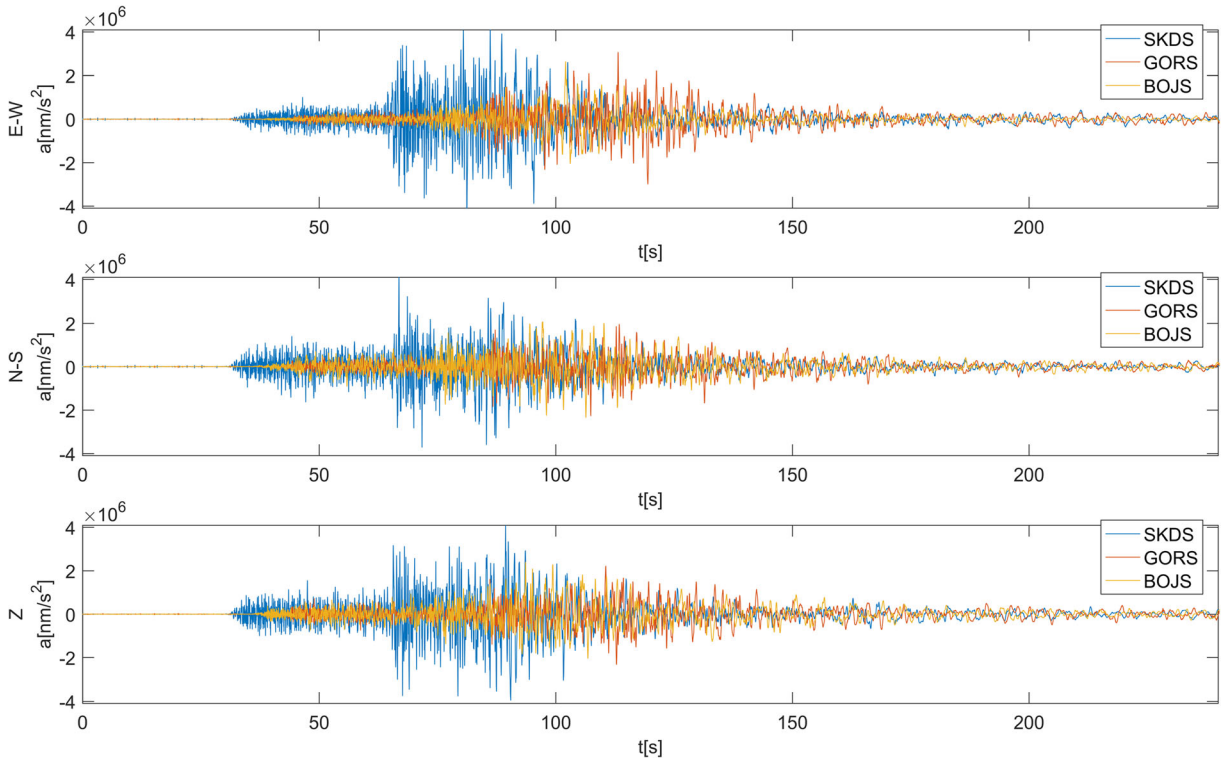

Fig. 6 As in Fig. 5, only the ground movements were detected by accelerometers

detection of accelerometer into the space of the detection of seismometer, is

$$\mathbf{B} = \begin{bmatrix} 0.98692 & 0.00758 & -0.00075 \\ -0.00667 & 0.98495 & -0.00773 \\ -0.00019 & 0.00893 & 0.98731 \end{bmatrix}.$$

From the transformation matrix **B**, various parameters can be estimated (Tasič and Runovc 2013). The calculated Euler angles are $\psi = -0.86°$, $\theta = -0.52°$, and $\phi = 1.25°$; the (horizontal) misalignment error, calculated by using Euler angles, is $\Delta\alpha = -0.39°$. The absolute value of Euler angle $|\theta|$ is also information about the angle between the vertical components of both systems. If it is small enough, then the (horizontal) misalignment error is $(-\psi - \phi)$ and represents the angle between the E-W components of both systems. All other calculated orthogonal deviations (or non-orthogonality) are around 0.1°. The orthogonal deviations do not affect the calculation; they can be even greater, as long as both systems are linear. The sensitivity corrections are $\mathbf{g} = [0.99\ 0.99\ 0.99]^{\mathrm{T}}$. The determinant of 3×3 transformation matrix $\mathbf{B}_g$ is $|\det(\mathbf{B}_g)| = 1.000002$ and $\Delta b_{\max} =$ 4e−05. Figure 8 presents PSD for both systems and the accelerometer's self-noise obtained from these seismic data. In the frequency range between 0.2 and 0.5 Hz, the PSD of seismic signal is approximately 30 dB over the signal of accelerometer's self-noise, which is acceptable. Experience shows that when the difference is less than 25 dB, the estimated results are questionable as the uncorrelated part of the signal (self-noise) cannot be neglected anymore.

Figure 9 presents PSD for both systems and the accelerometer's self-noise obtained from the record "January 18, 2017" (see also Figs. 3 and 4). The outputs for this record are $\mathbf{g} = [0.99\ 0.99\ 0.99]^{\mathrm{T}}$, $\Delta\alpha = -0.34°$, $|\det(\mathbf{B}_g)| = 1.000007$, and $\Delta b_{\max} = 2e-4$. The indicators $\det(\mathbf{B}_g)|$ and $\Delta b_{\max}$ are slightly worse, but they are acceptable. The absolute value of Euler angle $|\theta|$ is 0.57°. Misalignment errors differ for a 0.05° regarding to estimated value from the "October 30, 2016" record, but this is negligible. These small differences can come out as the result of different input data. The stronger the seismic signal is, with respect to the self-noise, on the assumption that the amplitude does not exceed the upper limit dynamic range of seismometer, the more accurate the calculated parameters should be. But this assumption is not real. In the case of larger ground movements, non-linear phenomena of the

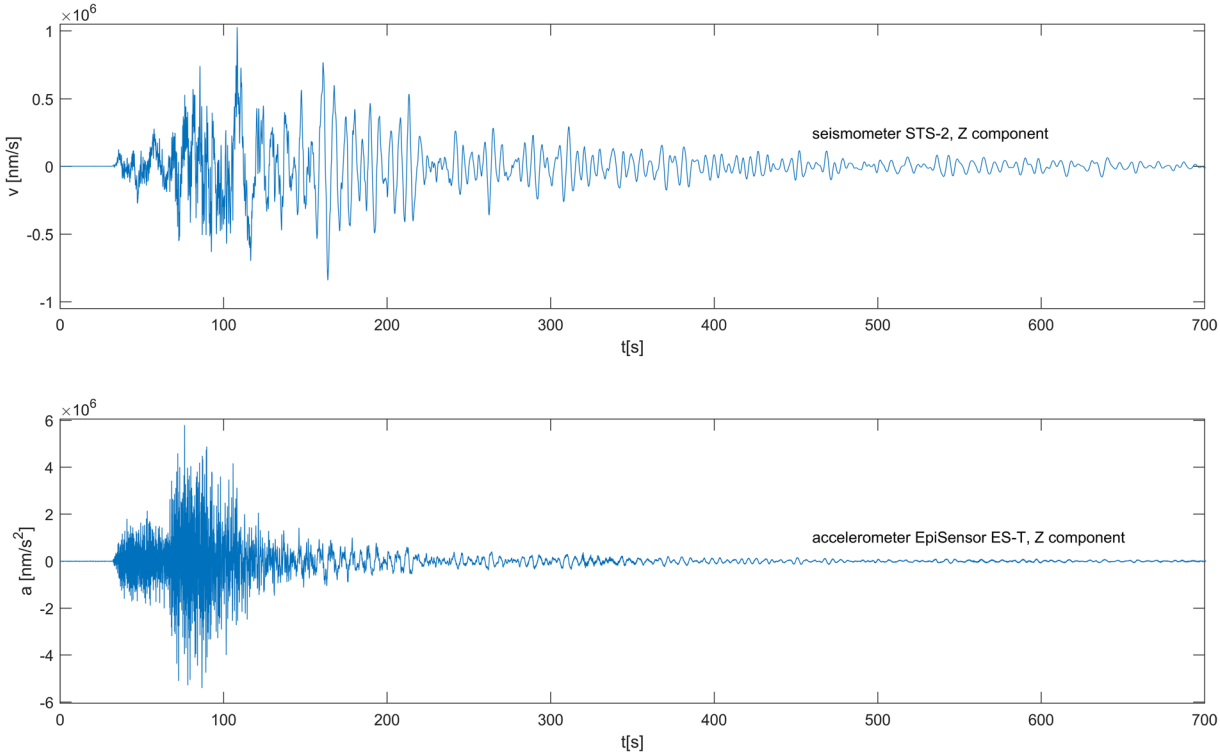

Fig. 7 Earthquake, located in central Italy (Mw = 6.5), recorded on October 30, 2016 by the station SKDS at the distance of 308 km. The upper plot represents the vertical record (first 4 min) at STS-2 seismometer, and the lower one represents the vertical record (first 4 min), registered by the accelerometer EpiSensor

measuring system can affect the measurements (e.g., Graizer 2009) and consequently the accuracy of the calculated parameters can be lower. This is valid for the estimated angles. The angle of misalignment error $\Delta\alpha$ is written to two decimal places, which is, according to the quality of data, too precise. Due to the little known influence of non-linear phenomena on seismometer at particular measurements, we can conclude that the misalignment error is between $-0.3°$ and $-0.4°$, and the difference in (vertical) leveling between seismometer and accelerometer is 0.5°.

Table 1 shows the estimated parameters for the location SKDS for all four records, including records "August 24, 2016" and "October 26, 2016." For the purpose of this study, sensitivity corrections, "misalignment error α" and "difference in leveling $|\theta|$" are written with greater accuracy, than it actually makes sense. The spectra ratio $P_{r_{qi}r_{qi}}/4\pi^2\nu^2 P_{q_iq_i}$ (Fig. 10) is consistent for all four events.

When we want to perform a quality control at a larger number of seismic stations, it is sufficient to check only the most important data. These are sensitivity corrections, "misalignment error," determinant of matrix $\mathbf{B}_g$, and Δb_{max}. The example of this is the seismic stations GORS. When estimated parameters deviate from the expected values, a more detailed analysis of the records and PSDs is needed. Such examples are in the next chapter.

The seismic station GORS is equipped with the seismometer CMG-3T (To = 360 s) and the accelerometer EpiSensor. Both are installed side by side and connected to the Q330HRS acquisition unit. The seismic station GORS is farther from earthquakes in central Italy than SKDS. The epicentral distance between the strongest earthquake in central Italy (Mw = 6.5, October 30, 2016) and the location GORS is 392 km. All estimated parameters (Table 2) are acceptable, and there is no need to perform a more detailed analysis of records. Hence, it follows that at this seismic station, the misalignment error between the accelerometer and the seismometer is 1.3° and the sensitivity corrections is $\mathbf{g} = [\ 0.99\ \ 0.98\ \ 0.99]^T$. The difference in leveling between the seismometer and accelerometer is 0.4°.

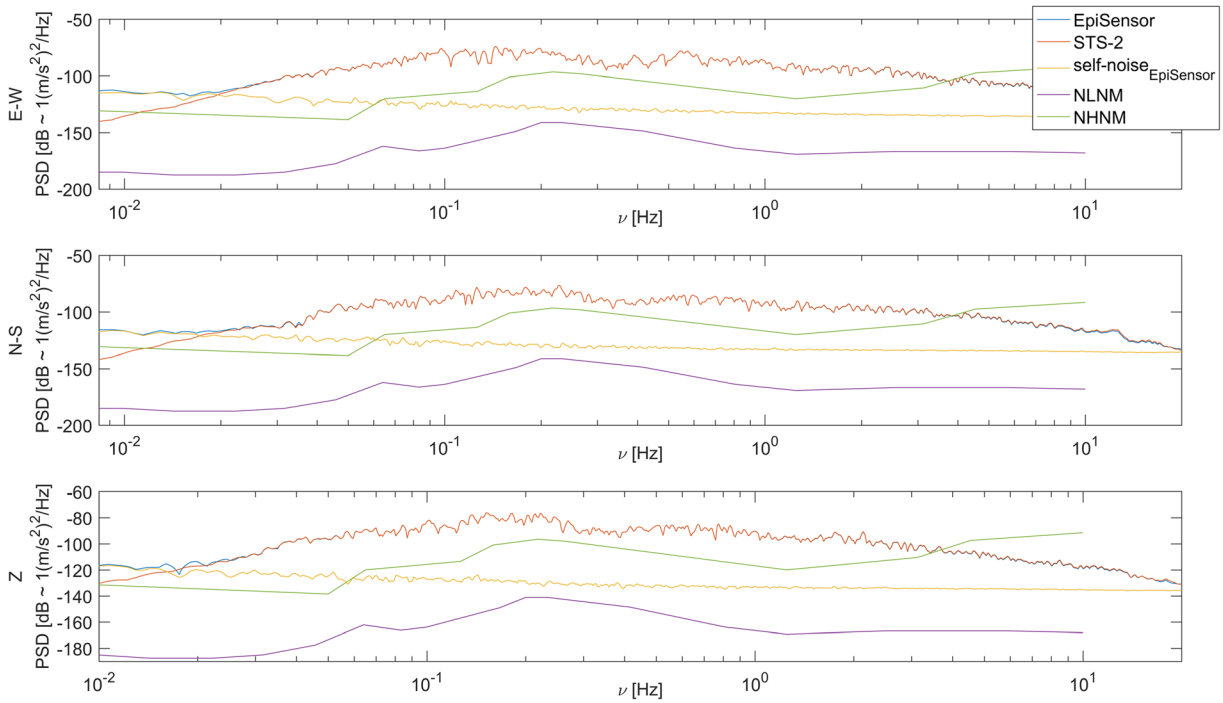

Fig. 8 PSD plots for the event "October 30, 2016" and estimated accelerometer's self-noise (see legend) for the site SKDS. For better representation, the PSD plots are smoothed

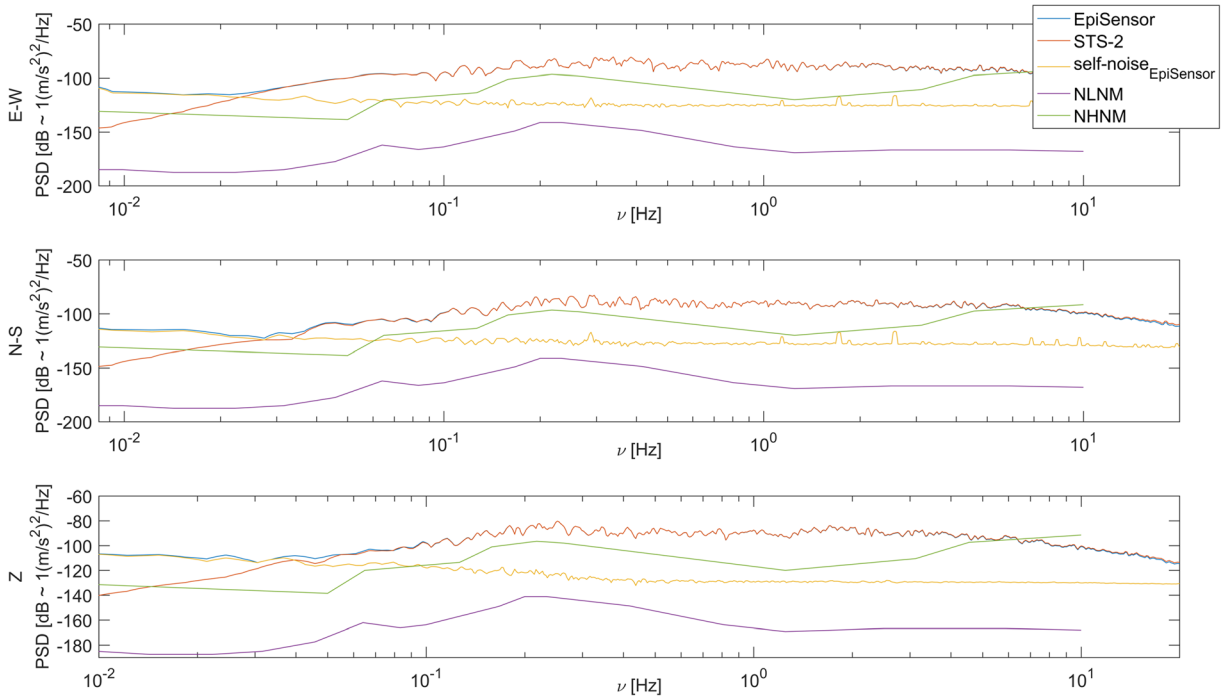

Fig. 9 PSD plots for the event "January 18, 2017" and estimated accelerometer's self-noise at seismic station SKDS. PSD plots are smoothed for clearer presentation

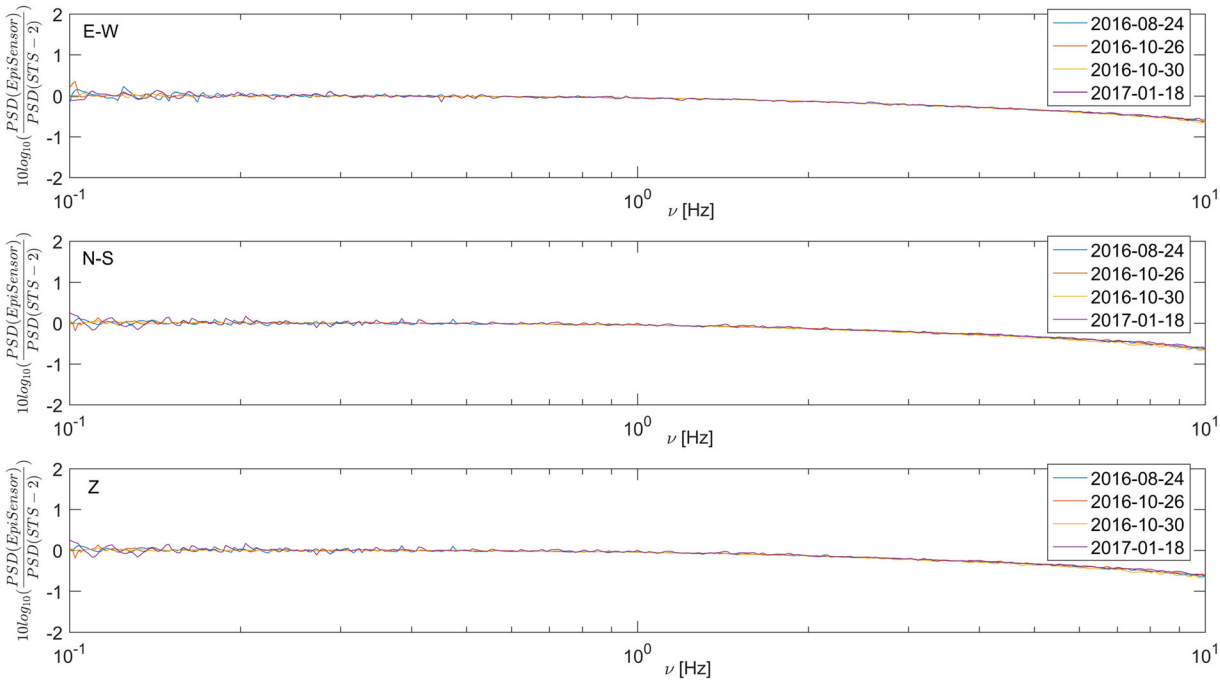

Fig. 10 PSD ratios ($P_{r_{qi}r_{qi}}/4\pi^2\nu^2P_{q_iq_i}$) between outputs of the STS-2 and the EpiSesor, for all four events. Instruments are installed side by side at the seismic station SKDS. Instrumental corrections were not included in the calculation

4 Error identification

The IQC of collocated seismometer and accelerometer is very useful for the systems, where the use of test signals, which are built into modern acquisition units, cannot identify all possible errors. An example of this is the failure of one piece of the equipment at the seismic station BOJS. This seismic station is located 90 km south from SKDS and has the same type of instruments as SKDS. At the beginning of September 2016, the IQC was performed with the data from the Italian earthquake ("August 24, 2016," Mw = 6.2). Estimated parameters were acceptable (Table 3). At the end of September, the seismometer STS-2 was tested with three different test signals, built into the Q330HRS acquisition unit. The test signals were "step," "sinus 1 Hz," and "white noise." The output signals in XYZ space were captured by the acquisition unit, transformed back to "UVW" space and analyzed. The responses to the test signals were correct for all three sensors and no error was identified. In October 2016, the IQC was performed on the data from the Italian earthquake (Mw = 6.1), which occurred in October 26, 2016. The results were unusual, the indicators were too high, and the value of "sensitivity correction" for E-W component was unusual (Table 3). The closer look at original E-W records (Fig. 11) and PSD of original data (Fig. 12) indicate that the "generator constant" in the calibration table could be incorrect; however, it was OK. PSD ratio $P_{r_{qi}r_{qi}}/4\pi^2\nu^2 P_{q_iq_i}$ between the transformed data of accelerometer and seismometer (Fig. 13) reveals that at this location, at least one E-W component detects ground movement incorrectly. A thorough analysis of older data pointed out the error at the E-W (or *X*) component of seismometer. It has been present for several weeks. The analysis indicated that the E-W (or *X*) component of seismometer "leaks." The error occurred before the seismometer was tested by test signals. Why the test signals did not point out any error will be clarified with this simple mathematical approach. The equation

$$\begin{bmatrix} X \\ Y \\ Z \end{bmatrix} = \begin{bmatrix} -\sqrt{2/3}(h_U \otimes x_t) + \sqrt{1/6}(h_V \otimes x_t) + \sqrt{1/6}(h_W \otimes x_t) \\ \sqrt{1/2}(h_V \otimes x_t) - \sqrt{1/2}(h_W \otimes x_t) \\ \sqrt{1/3}(h_U \otimes x_t) + \sqrt{1/3}(h_V \otimes x_t) + \sqrt{1/3}(h_W \otimes x_t) \end{bmatrix} \tag{14}$$

represents a theoretical transformation matrix (e.g., Streckeisen 1995), which transforms responses of

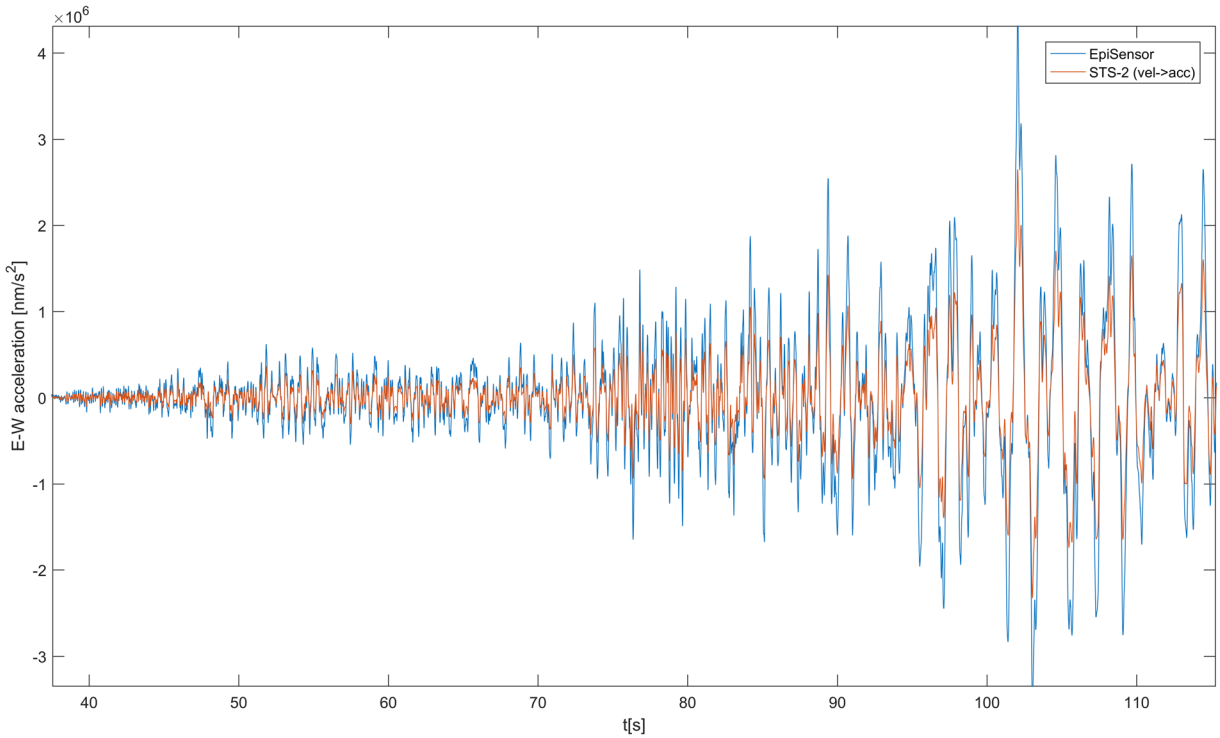

Fig. 11 E-W waveforms of the regional earthquake ("October 26, 2016," central Italy), detected by the seismometer STS-2 and the accelerometer EpiSensor at the seismic station BOJS. They should detect equally moderate shaking of the ground, but E-W records differ from each other. The reason is the defective seismometer cable. See also Figs. 12 and 13

sensors U, V, and W to the calibration signals x_t into the Cartesian XYZ space. The differences in the transfer functions are assumed to be negligibly small ($h_U \approx h_V \approx h_W = h$) as the identical design for all three sensors in Galperin configuration is essential for the proper detection of ground motion (e.g., Townsend 2014, Graizer 2009). By using this, responses to the test signals were recorded only at Z component

$$\begin{bmatrix} X \\ Y \\ Z \end{bmatrix} = \begin{bmatrix} 0 \\ 0 \\ h \otimes x_t \end{bmatrix}. \tag{15}$$

We can see that faults, which exist only at X and/or Y line (e.g., are behind the sensors), cannot be identified with test signals.

The cable between STS-2 and HostBox was found as a source of error, due to electro corrosion between the pins of connectors. The cable was replaced by a new one. During the replacement process, the threat of rain increased, the operators were careless, and the seismometer was shifted slightly. The misalignment error increased for more than 11° (Table 3). This error was again identified by the IQC approach, performed a few days later, on the record from the central Italian earthquake (Mw = 6.5, October 30, 2016, the epicentral distance was 341 km). Without IQC, the deviation of 11.3° between the two systems can be easily overlooked. Even if the record from the seismometer is converted to the acceleration record (Fig. 14), it is still possible that the user cannot notice such differences in the graphs without any additional warning. Being warned about this error, the seismometer was reoriented by the operators. Now, the orientation misalignment is − 1.6° (Table 3).

5 Discussion

This novel procedure enables the precise evaluation of the operational quality of collocated seismometer and accelerometer. A moderate shaking of the ground in the frequency interval where both instruments have flat transfer functions, a "seismometer is not yet clipped" and an accelerometer is also capable to detect it, is needed. It is important that both systems detect equal moderate shaking of the ground. This "equal" moderate

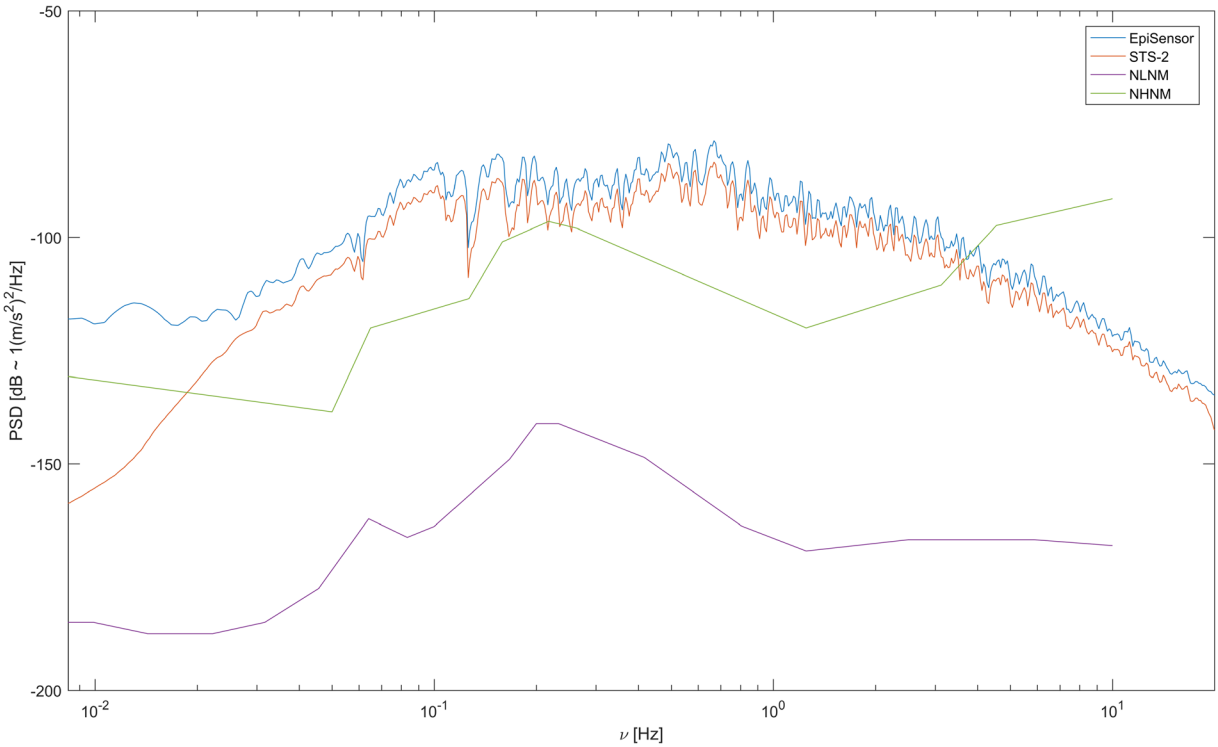

Fig. 12 PSD view of the event "October 26, 2016" for the (original) E-W component of accelerometer (blue line) and seismometer (red line), both installed at the location BOJS. The difference in PSD graphs indicates that the data in the calibration table could be incorrect. But the reason of the error was a defective seismometer cable (see also Fig. 11 and 13). PSD plots are smoothed for clearer presentation

shaking is usually a result of stronger regional earthquakes or moderate local earthquakes. The IQC procedure is based on the calculation of transformation matrix which numerically transforms the detection of accelerometer into the space of the detection of seismometer. The input data in the procedure are the same as those recorded on individual systems (in the sense of units). The matrix can be adequately calculated if, in the frequency interval between 0.2 and 0.5 Hz, the PSD of seismic signal is above the self-noise of the accelerometer for at least 25 dB. If it is not, the influence of uncorrelated signal cannot be neglected in the Eq. (8). The "=" in this equation is changed to "<" and the procedure, described in this paper, is not valid any more. Following that, we were unable to adequately calculate the transformation matrices in any other way, than by seismic signals of stronger regional earthquakes. Some other sources of seismic signals, such as secondary microseism or local "seismic noise," were tested too. But, as the signals were not strong enough in a requested frequency interval, we were unable to obtain reliable information.

The equal and moderate shaking of the ground could be (theoretically) caused also by man-made sources. It is important that the shaking is exactly the same for both systems and is strong enough that the PSD of detected signal is above the self-noise of accelerometer for at least 25 dB.

The duration of a seismic signal is also important: the longer the duration of the signal is, the better and more accurate are calculated data. The signal from regional earthquakes represents a restriction, because of limited duration. In observed examples, the data length was between 20 and 60 min and PSDs were approximately between 25 and 35 dB above the self-noise of accelerometers.

The influence of the length of a record on the estimated parameters was also tested too. For the seismic station GORS, a 3-h series were available for all four events. The start of the earthquake is in the first recorded minute at all four records. Initially, the first 5 min are used for each event. At first, all necessary parameters are calculated for these (5 min) records, including $|\det(\mathbf{B}_g)|$ and $\Delta b_{\max}$. Next, each record is increased by 1 min. All

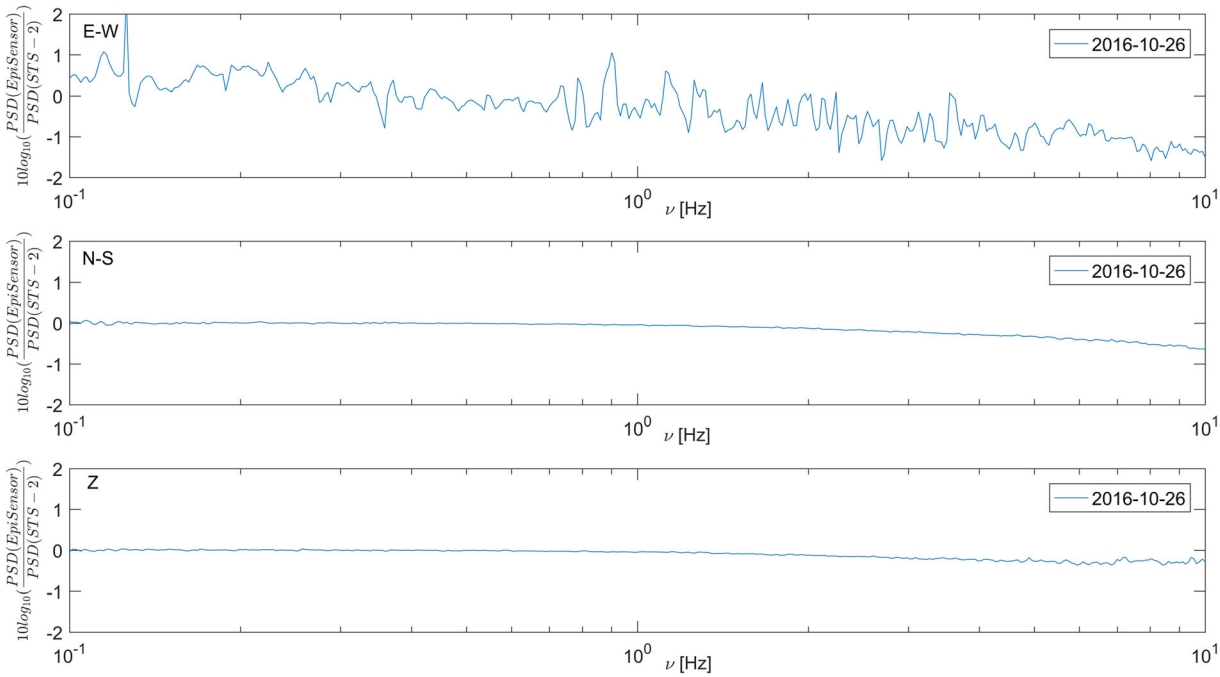

Fig. 13 PSD ratio between the outputs of the STS-2 seismometer and of the EpiSensor accelerometer, for the event "October 26, 2016." Both systems are installed side by side at the location BOJS. PSD ratio for E-W component indicates that irregularities in the data are not connected to the parameters in the calibration files. Otherwise, the ratio for E-W should be similar to the ratio for N-S and Z

steps were repeated again until the end of the record was reached. For all events, it has turned out that the length of records should not be shorter than 18 min. If they are shorter, the estimated parameters significantly deviate from the expected values. The same follows if records are too long. Records for events of 2016 can be an hour long, and estimated parameters are still inside the expected values. The record for the event "January 18, 2017" needs to be shorter. Its length should not exceed 35 min. Within the "allowed" interval, the sensitivity corrections remain the same and $\Delta\alpha$ are between 1.27° and 1.33°. For all events, the optimum record's lengths are defined too. For a particular event, the optimal record's length is defined by the record, whose products of estimated parameters $|\det(\mathbf{B}_g)|$ and Δb_{max} are the smallest. Estimated parameters of these records are in Table 4.

For the sake of the above, we can be relatively superficial in choosing the length of the recorded event, and because of this, the IQC can be performed automatically at several seismic stations located within a relatively large area.

Because of the Eq. (5), the length of input data and the sampling rate need to be equal. But in some seismic arrays, different sample rates are used for seismometers and accelerometers. To perform IQC, the data, which is sampled faster, needs to be decimated. It is important that the data in the frequency range between 0.2 and 0.5 Hz is not affected by this procedure. We took a test for the event "October 30, 2016" for the location KNDS, where a record from a seismometer, sampled with 20 sps, was available. We resampled a record from the accelerometer from 200 to 20 sps (by using the built-in function in MatLab) and re-calculated the parameters. The new parameters are within the expected values. The misalignment error is $\Delta\alpha = -0.39°$. The sensitivity corrections are $\mathbf{g} = [\,0.988\ 0.986\ 0.988]^T$. The determinant of 3×3 transformation matrix $\mathbf{B}_g$ is $|\det(\mathbf{B}_g)| = 1.000001$ and $\Delta b_{max} = 1e{-}04$.

The main disadvantage of this method is its dependence on unpredictable strong regional earthquakes. On the other hand, this procedure has many advantages. Transformation matrix contains a lot of important information (Tasič and Runovc 2012, 2013), such as orientation misalignment and sensitivity corrections. Interdependent quality control of collocated seismometer and accelerometer is also important to detect errors. This process plays an important role at triaxial seismometers

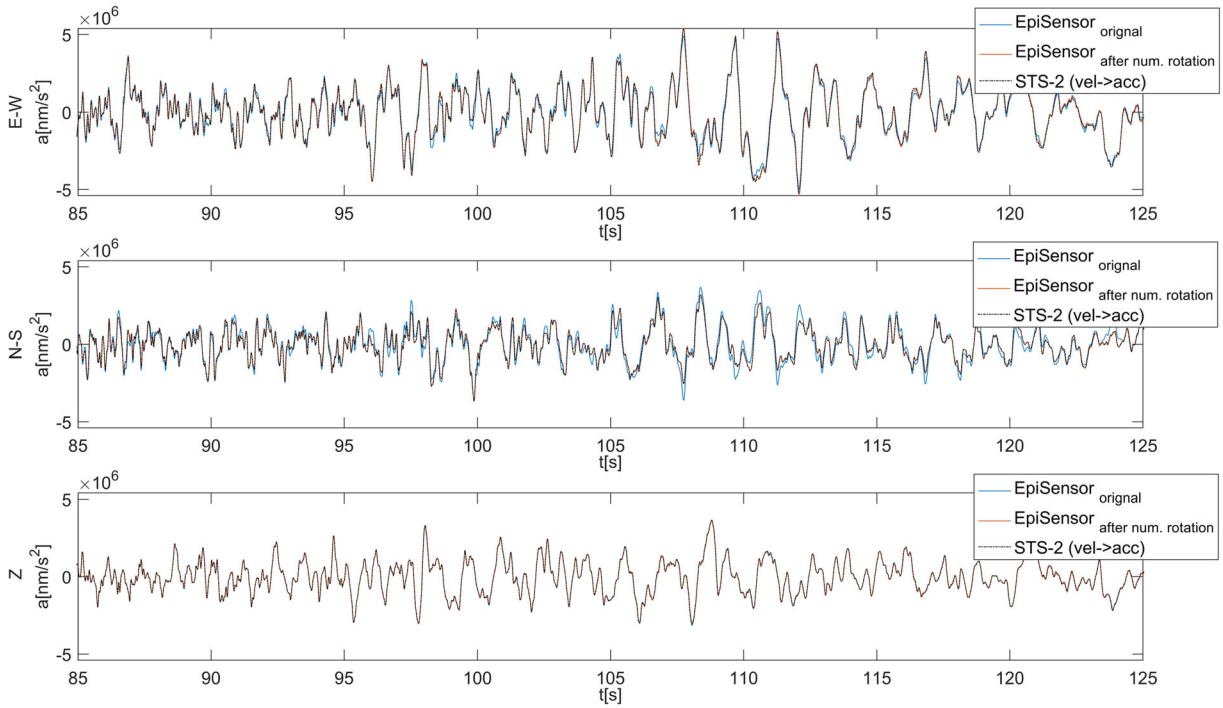

Fig. 14 The seismic station BOJS, event "October 30, 2016": interval with the largest amplitudes. It is difficult to manually estimate the source of small difference between plots (between blue full and black striped line) at E-W and N-S components from the original records. Such information is obtained from the transformation matrix **B**: the difference between plots is due to the orientation misalignment which is 11.3°. For comparison, an acceleration record is presented (red line), after it was numerically transformed (rotated) to the space of seismometer

with Galperin arrangement (or "symmetric triaxial" design). Some errors at E-W or N-S component cannot be identified with the calibration signals and built-in modern acquisition units, if test signal are initiated into all three components with the same amplitude at the same time. When this type of a seismometer is installed side by side with an accelerometer, such errors can be identified by the method, described here.

The indicators $|\det(\mathbf{B}_g)|$ and Δb_{max} are very useful. However, their values are more indicative and some experience is needed to determine a threshold level. When any of estimated parameters deviate from the expected one, a manual comparison of records in the time domain needs to be performed. To check records of both units manually, either the data from a seismometer have to be converted into acceleration or the data from accelerometer have to be converted to velocity. In the first case, numerical differentiation has to be performed and one sample is lost. In the second case, the self-noise of accelerometer is still presented at low frequencies, and additional filtering is needed for the converted data to minimize the long period disturbances. Because on this, small deviations can be overlooked during the manual comparison of records. Therefore, it is

Table 4 Four records from regional earthquakes, detected at location GORS, were used again (as in Table 2); only this time, the optimal length ($L_{optimal}$), instead of the original one, is estimated for each record and used in calculation

Date of the earthquake	Mw	g_{EW}	g_{NS}	g_Z	α	$\lvert\theta\rvert$	$\lvert\det(\mathbf{B}_g)\rvert$	Δb_{max}	$L_{optimal}$ (min)
2016 August 24	6.2	0.991	0.983	0.994	1.30°	0.36°	1 + 9e−6	4e−05	43
2016 October 26	6.1	0.991	0.984	0.995	1.29°	0.41°	1 + 11e−6	3e−05	29
2016 October 30	6.5	0.991	0.984	0.995	1.30°	0.38°	1 + 9e−6	3e−05	47
2017 January 18	5.7;5.6	0.989	0.982	0.993	1.30°	0.41°	1 + 9e−6	1e−04	29

recommended that transformed acceleration data $\tilde{\mathbf{y}}_r$ are also used simultaneously in this control (Fig. 14).

At the end of the year 2016, seismometers and accelerometers were installed side by side at 14 seismic stations of the Seismic Network of the Republic of Slovenia. Using the described procedure, some irregularities were discovered. Some examples were already described (seismic station BOJS; Section 4). At location, where a seismometer and an accelerometer were attached to the different acquisition units, small deviations in time were discovered. The producer of the critical acquisition unit was informed and has already sent correction (upgrade). However, one additional larger misalignment error was also discovered too. It was in the range of 7.1°. The accelerometer was incorrectly oriented.

6 Conclusion

The number of seismic stations, where a broadband seismometer and strong-motion accelerometer are installed side by side, is rising. The number of instruments, needed to be controlled, is greater and leads to more activities, related to the quality control. With the Interdependent quality control both instruments are controlled simultaneously and the defects or other problems on instruments can be identified. Procedures can be automated. The IQC is suitable for a large number of seismic stations. But it can only be used, when both systems detect equal moderate shaking of the ground. At our locations, the source of shaking was only strong regional earthquakes. This is also the main disadvantage of the described method; it depends on unpredictable strong regional earthquakes. On the other hand, this procedure has many advantages, such as detection of different errors.

Further studies of different locations and different instruments will be needed to define the permitted levels for sensitivity corrections and "orientation misalignment." The obtained information will make the decision to act in a particular location easier.

The additional studies with local earthquake waveforms will also be needed, since the amplitude of shaking of the ground is the largest in the frequency interval, where the transfer functions of seismometers and accelerometers are not flat anymore, and this affects the accuracy of the calculated data. This data could be calibrated according to the values previously obtained from the strong regional earthquakes. Using local earthquakes would make the procedure even more useful.

Acknowledgments We thank the Slovenian Environment Agency (ARSO) for making the measurements possible. The author would like to express his gratitude to both anonymous reviewers for their constructive and useful comments and advice.

References

Borman P (2002) Seismic signal and noise. In: Borman P (ed) New manual of seismological observatory practice, vol 1. GeoForschungsZentrum, Potsdam

Collette C, Carmona-Fernandez P, Janssens S, Artoos K, Guinchard M, Hauviller C (2011) Review of sensors for low frequency seismic vibration measurement, ATS/Note/2011/001 (TECH); https://cds.cern.ch/record/1322403/files/CERN-ATS-Note-2011-001-TECH.pdf

Graizer V (2009) The response to complex ground motions of seismometers with Galperin sensor configuration. Bull Seismol Soc Am 99:1366–1377

Holcomb GL (1989) A direct method for calculating instrument noise levels in side-by-side seismometer evaluations. Open-file report 89-214, U. S. Geological Survey

Holcomb GL (1990) A numerical study of some potential sources of error in side-by-side seismometer evaluations. Open-file report 90-406, U. S. Geological Survey

Holcomb GL (2002) Experiments in seismometer azimuth determination by comparing the sensor signal outputs with the signal output of an oriented sensor. Open-file report 02–183, U. S. Geological Survey

Pavlis GL, Vernon FL (1994) Calibration of seismometers using ground noise. Bull Seismol Soc Am 84(4):1243–1255

Peterson J (1993) Observations and modeling of background seismic noise. Open-file report 93-322, U. S. Geological Survey

Ringler AT, Hutt RC (2010) Self-noise models of seismic instruments. Seismol Res Lett 81:972–983

Ringler AT, Evans JR, Hutt RC (2015) Self-noise models of five commercial strong-motion accelerometers. Seismol Res Lett 86:1143–1147

Rodgers PW (1992) Frequency limits for seismometers as determined from signal-to-noise ratios. Part 2. The feedback seismometer. Bull Seismol Soc Am 82:1099–1123

Sleeman R, Melichar P (2012) A PDF representation of the STS-2 self-noise obtained from one year of data recorded in the Conrad observatory, Austria. Bull Seismol Soc Am 102: 587–597

Sleeman R, van Wettum A, Trampert J (2006) Three-channel correlation analysis: a new technique to measure instrumental noise of digitizers and seismic sensors, Bull Seismol Soc Am 96(1): 258–271

Streckeisen G (1995) Portable Very Broad Band Tri-Axial Seismometer, STS-2 manual, Tech. Rep., G. Streckeisen AG, Pfungen, Switzerland

Tasič I, Runovc F (2012) Seismometer self-noise estimation using a single reference instrument. J Seismol 16:183–194. https://doi.org/10.1007/s10950-011-9257-4

Tasič I, Runovc F (2013) Determination of a seismometer's generator constant, azimuth, and orthogonality in three-

dimensional space using a reference seismometer. J Seismol 17:807–817. https://doi.org/10.1007/s10950-012-9355-y

Tasič I, Runovc F (2014) The development and analysis of 3D transformation matrices for two seismometers. J Seismol 18: 575–586. https://doi.org/10.1007/s10950-014-9429-0

Townsend B (2014) Symmetric triaxial seismometers. In: Michael B, Ioannis KA, Edoardo P (eds), Encyclopedia of Earthquake Engineering, https://doi.org/10.1007/978-3-642-36197-5_194-1

Welch PD (1967) The use of fast Fourier transform for the estimation of power spectra: a method based on time averaging over short, modified periodograms IEEE Trans Audio Electroacoust, AU-15 (1967), pp. 70–73

Wielandt E (2002) UNICROSP. In: Bormann P (ed) New manual of seismological observatory practice (NMSOP), volume 2, annexes, GeoForschungsZentrum, Potsdam:PD 5.7,1–2Potsdam